microbiology research

MDPI

Article

Study of the Relationship Between Natural Mating Expression and Intestinal Resistance Genes in Captive Adult Giant Pandas

Ming-Yue Zhang [1,2,3,*], Xiao-Hui Zhang [1,2], Xue-Ying Wang [1], Jun-Hui An [1,2,3], Dong-Hui Wang [1,2,3], Rong Hou [1,2,3] and Yu-Liang Liu [1,2,3,*]

[1] Chengdu Research Base of Giant Panda Breeding, Chengdu 610081, China; xiaohuizhang1986@163.com (X.-H.Z.)
[2] Sichuan Key Laboratory of Conservation Biology for Endangered Wildlife, Chengdu 610081, China
[3] Sichuan Academy of Giant Panda, Chengdu 610081, China
* Correspondence: zmy6611@126.com (M.-Y.Z.); liuyuliang@panda.org.cn (Y.-L.L.); Tel.: +86-17742851501 (M.-Y.Z.); +86-13568876372 (Y.-L.L.)

Abstract

A growing body of evidence indicates that the gut microbiota has a role in the mating preference process in mammals. This likely occurs through the modulation of various mating signals induced by symbiotic bacteria, thereby leading to variations in mating behavior. Given that giant pandas are solitary wild animals that rely on chemical signals for mate selection, it is relevant to explore whether the mating behavior of giant pandas is also affected by the gut microbiota. We hypothesize that antibiotic treatment-induced residual antibiotic resistance genes in captive giant pandas may disrupt intestinal microbiota homeostasis, diminish the abundance of beneficial microorganisms involved in short-chain fatty acid synthesis, and consequently impair nervous system function via the gut–brain axis. The ensuing physiological stress is likely to suppress innate mating behavior and compromise pheromone synthesis, thereby reducing an individual's attractiveness to potential mates. To answer this question, we utilize fecal metagenomics technology to analyze the differences in gut microbes and antibiotic resistance genes (ARGs) between captive male adult giant pandas displaying natural versus non-natural mating behavior. The research findings suggest that, when compared with captive adult male giant pandas demonstrating natural mating behavior, those with non-natural mating behavior exhibit a significantly reduction in the abundance of beneficial gut microorganisms (*s_Clostridium* sp. and *f_Ruminococcaceae*) ($p < 0.05$). Concurrently, there is a significantly increase in the observed resistance genes *tetO* and *mgtA*, which are mainly associated with macrolide and tetracycline resistance ($p < 0.05$). Furthermore, Kegg functional analysis reveals a significant up-regulation of metabolic pathways related to sensory systems, such as taste and olfactory transduction, in the intestines of captive adult male giant pandas showing natural mating behavior. These results imply that changes in the abundance of gut microbiota and ARGs are correlated with the manifestation of natural mating behavior in captive adult male giant pandas. Consequently, to improve the success rate of natural reproduction within the male giant panda populations in captive environments, it is advisable to administer antibiotics judiciously and closely monitor the composition of beneficial bacteria in their gut microbiota. The findings of this study provide novel perspectives on the mechanisms by which captive conditions affect the decline in natural mating behavior observed in adult male giant pandas.

Check for updates

Academic Editor: Vincenzo Cuteri

Received: 9 January 2026
Revised: 14 February 2026
Accepted: 15 February 2026
Published: 18 February 2026

Copyright: © 2026 by the authors. Licensee MDPI, Basel, Switzerland. This article is an open access article distributed under the terms and conditions of the Creative Commons Attribution (CC BY) license.

Keywords: giant panda (*Ailuropoda melanoleuca*); natural mating behavior; gut microbiota; antibiotic resistance genes

1. Introduction

The gut microbiota assumes a pivotal role in mediating the interaction between the host and its environment, exerting a wide array of effects on the behavior of animals [1]. For example, it can engage in intricate crosstalk with the host to produce intermediary or end products of microbial metabolism, such as short-chain fatty acids (SCFAs) [2]. By harnessing these metabolites, the gut microbiota enables bidirectional communication between the brain and the intestine via pathways associated with gut SCFAs and tryptophan metabolism, thereby influencing host physiology and behavior [3]. Although the impact of gut microbiota on insect mating behavior has been extensively documented, investigations into its influence on mammalian sexual attraction and mate selection remain limited. It has recently been reported that gut microbiota dysbiosis can reduce the sexual attraction of female mice to male mice (Mus), indicating a potential role of symbiotic gut microbiota in modulating mammalian mate selection behavior [4]. However, there is a dearth of research regarding large mammals such as the giant panda (*Ailuropoda melanoleuca*).

The gut microbiota is recognized as a reservoir of ARGs. The structure of the microbiota is associated with the composition of ARGs. The stability of the gut microbiota constitutes the core of host health. Antibiotic exposure, meanwhile, is a crucial factor that disrupts the balance of the gut microbiota [5]. At present, antibiotics are the primary drugs employed for treating bacterial infections in giant pandas. Antibiotics exert their therapeutic effects by directly killing pathogenic bacteria or inhibiting their growth. Numerous studies have revealed that the intestines of captive giant pandas harbor multiple rich reservoirs of ARGs and serve as hubs for horizontal gene transfer [6]. Recent studies show that antibiotic exposure in pandas may also originate from their bamboo diet [7]. In mammalian research, it has been demonstrated that under captive conditions, the continuous pressure of low-dose antibiotics can result in dysbiosis of the gut microbiota and facilitate the horizontal gene transfer of ARGs in commensal bacteria. This microecological disruption is far more detrimental than simply inducing infections. Its harm lies in functional impairments, specifically the weakening of key capabilities such as the synthesis of SCFAs, the regulation of bile acid metabolism, and the production of neuroactive substances (such as serotonin and γ-aminobutyric acid) [8]. These microbial metabolites are the core messengers in the "gut–brain axis" communication and directly or indirectly modulate the function of the hypothalamic–pituitary–gonadal axis (HPG axis) [9].

The administration of antibiotics can perturb the composition of the gut microbiota, thereby disrupting its homeostatic equilibrium and fostering the expansion of drug-resistant bacterial populations. Such perturbations not only compromise the protective role of the microbiota but also heighten host susceptibility to drug-resistant pathogens, diminish microbial diversity, and alter the abundance and metabolic activity of bacterial communities [10]. Furthermore, antibiotic usage promotes the dissemination of antimicrobial resistance genes and adversely affects the structural and functional integrity of the gut microbiota. For example, β-lactam antibiotic therapy is frequently associated with a marked reduction in microbial diversity and metabolic functionality [11]. Antibiotic-induced dysbiosis can also severely impair the metabolic and immunomodulatory functions of the gut microbiota. Clinical observations indicate that such dysbiosis leads to a decline in beneficial bacteria alongside an expansion of pathogenic species [12]. This imbalance correlates with

decreased concentrations of short-chain fatty acids and tryptophan, as well as elevated levels of purines.

The giant panda, a flagship species for global biodiversity conservation, is a rare species endemic to China [13]. Besides in situ conservation, ex situ conservation also plays a crucial role in the protection of endangered wildlife [14]. The implementation of the ex situ conservation and breeding program for giant pandas has achieved phased successes in their conservation [15]. In captive settings, giant pandas frequently display a decrease in natural mating behavior [16], which is likely due to the restriction of their free mate choice imposed by the captive environment [17]. Giant pandas are highly selective, solitary foragers [18]. In the brief spring estrus period, wild individuals primarily utilize chemical cues from perianal gland secretions and urine to disseminate reproductive signals and facilitate mate choice [19,20]. Consequently, mate selection represents a critical stage in the giant panda mating process, directly influencing the likelihood of successful natural copulation between males and females. This process holds significant implications for the management of captive populations and the recovery of small, isolated wild populations [21,22]. Nevertheless, in the managed captive setting during the breeding period, not only does it restrict the freedom of mate choice among giant pandas, but also disinfection and sterilization of enclosures, along with antibiotic treatment for diseases, inevitably disrupts the original balance of the intestinal microbiota in wild animals, affecting the composition and dissemination of intestinal microbiota [6]. Research on mouse has demonstrated that gut microbiota can influence the synthesis of sex pheromones, which in turn impacts their mating choice behavior [5]. Given that giant pandas, as solitary wild animals, rely on chemical signals for mate selection, could the natural manifestation of mating behavior in captive adult male giant pandas be associated with changes in gut microbiota caused by unnatural environments?

We therefore hypothesize that the intensive administration of antibiotics in captive environments may induce gut microbiota dysbiosis in giant pandas, fostering the expansion of pathogenic bacteria while diminishing the abundance of microbial taxa involved in the synthesis of intestinal metabolites, such as short-chain fatty acids. These alterations are posited to impact nervous system function via the gut–brain axis, elicit psychological stress, and consequently suppress natural mating behavior and disrupt the synthesis of chemical pheromones, ultimately reducing an individual's sexual attractiveness to potential mates. To test this hypothesis, we selected captive adult male giant pandas exhibiting either natural or non-natural mating behavior from the Chengdu Research Base of Giant Panda Breeding as our study cohort. Metagenomic sequencing of fecal samples was performed to elucidate the relationship between gut microbial composition, antibiotic resistance gene abundance, and mating behavior from an intestinal microbiological perspective. This approach offers a novel avenue for uncovering the physiological mechanisms through which captive conditions influence mate choice and natural mating behavior in giant pandas.

2. Materials and Methods

2.1. Sample Collection

Eleven healthy captive adult male giant pandas from the Panda Base were selected as the research subjects (sample details were presented in Table 1). The feeding protocol for all these animals, spanning from birth to adulthood, was consistent, and the diet provided at different physiological stages was standardized. Throughout adulthood, all of the experimental giant pandas were maintained in solitary confinement. Moreover, all the giant pandas had undergone tetracycline antibiotics treatment (chlortetracycline hydrochloride) during their infancy. Although the gut microbiota of young animals was vulnerable to alterations induced by various external factors, it became stable in adulthood [23].

After rigorously controlling for influencing factors of gut microbiota and ARGs (such as age, diet, prior antibiotic treatment, etc.), the pandas were divided into two groups: the NM group, consisting of five male adult giant pandas with successful natural mating experience (able to produce offspring through natural mating after reaching adulthood) The artificial insemination (AI) group comprised six male adult giant pandas without successful natural mating experience (unable to produce offspring through natural mating after reaching adulthood). The specific groupings were shown in Table 1. Fecal samples were collected within ten minutes of defecation, with the outer layer of feces in contact with the ground being removed. The fecal samples were then placed in sterile bags, air was expelled, transported back to the laboratory in an ice box, and stored at −80 °C. The NM group yielded 13 fresh fecal samples while the AI group yielded 18 fresh fecal samples. All fecal samples of giant pandas were gathered during the estrus period in winter 2023 (February). Regarding the NM group, fecal samples were collected daily between 8:00 and 9:00 a.m. Specifically, fecal samples from four pandas were collected for three consecutive days, whereas samples from Xiang Ge was collected for one day. For the AI group, the collection methodology was identical to that of the NM group, and the collection time was also set from 8:00 to 9:00 a.m. Fecal samples from six pandas in this group were collected for three consecutive days.

Table 1. Basic information of the research object.

Group	Name	Whether Natural Mating Behavior Is Expressed Normally	Studbook	Birth Year	Sampling Time Points	Sampling Data
NM	Gong Zai	Yes	711	2008	3	2023.2.4–2023.2.6
NM	Mei Lan	Yes	649	2006	3	2023.2.4–2023.2.6
NM	Xiong Bang	Yes	540	2001	3	2023.2.4–2023.2.6
NM	Lou Abao	Yes	703	2007	3	2023.2.4–2023.2.6
NM	Xiang Ge	Yes	674	2007	1	2023.2.5
AI	Xi Lan	No	731	2008	3	2023.2.4–2023.2.6
AI	Ying Ying	No	724	2008	3	2023.2.4–2023.2.6
AI	Cheng Shuang	No	857	2012	3	2023.2.4–2023.2.6
AI	Xing Bang	No	614	2005	3	2023.2.4–2023.2.6
AI	Da Mao	No	732	2008	3	2023.2.4–2023.2.6
AI	Yuan Lin	No	788	2010	3	2023.2.4–2023.2.6

2.2. Total DNA Extraction and Database Construction

Owing to the high proportion of undigested bamboo in the feces of giant panda, a pre-treatment procedure was indispensable for the extraction of total DNA. Approximately 10 g of feces were transferred into a 10 mL centrifuge tube and combined with 8 mL of sterilized phosphate-buffered saline (PBS). The resulting mixture was then vortexed for 5 min to dissociate microorganisms from bamboo particles and other fecal components, after which the supernatant was collected. This process was repeated three times. Subsequently, microbial precipitates were obtained by centrifugation at 12,000 *g* for 10 min and stored at −70 °C. Total DNA was extracted from the precipitates using the Omega fecal DNA extraction kit (M4015-00, Norcross, GA, USA). The purity and integrity of the extracted DNA were analyzed via 1% agarose gel electrophoresis (AGE). DNA quantification was conducted using the Qubit ® DsDNA Assay Kit in a Qubit ® 2.0 Fluorometer (Life Technologies, Carlsbad, CA, USA). Samples were appropriately diluted with sterile water to attain an optical density (OD) value ranging from 1.8 to 2.0 [24].

A single sample of μ Genomic DNA was employed for library construction using the NEBNext® Ultra DNA Library Prep Kit for Illumina (NEB, Ipswich, MA, USA). The DNA was randomly fragmented to an approximate length of 350bp using a Covaris ultrasonic

crusher. The library was then prepared through a series of procedures, including end repair, A-tailing, addition of sequencing adapters, purification, and PCR amplification. After library construction, initial quantification was carried out using Qubit2.0 and the library was diluted to a concentration of 2 ng/uL. Subsequently, the Agilent 2100 system was utilized to evaluate the insert size of the library. Once the library inspection was successfully completed, the different libraries were pooled according to their effective concentrations and the requirements for the target offline data volume, followed by Illumina PE150 sequencing.

2.3. Sequencing Results Pretreatment

The preprocessing of raw data derived from the Illumina HiSeq sequencing platform was carried out using Readfq to acquire clean data for subsequent analysis. The detailed processing steps were as follows: (a) Removal of reads containing low-quality bases (quality score $\leq$ 38) that exceeded a specific proportion (default set to 40 bp); (b) Elimination of reads with a certain proportion of N bases (default set at 10 bp); (c) Exclusion of reads that had an overlap with the adapter exceeding a particular threshold (default set at 15 bp). When host contamination was detected in the sample, it was essential to compare with the host sequence and filter out reads potentially originating from the host. By default, Bowtie2 software was employed for this task [25].

2.4. Metagenome Assembly

The Clean Data were assemble and analyzed using MEGAHIT software (v1.0.4-beta). Subsequently, the assembled Scaffolds were fragmented at the N connections to obtain Scaffolds without N [26,27].

2.5. Gene Prediction and Abundance Analysis

Open reading frame (ORF) prediction was conducted on scaftigs (with a length of $\geq$500 bp) by means of MetaGeneMark [28]. To refine the initial output, sequences shorter than 100 nt were subsequently removed [29]. Thereafter, CD-HIT was employed to reduce the redundancy in the predicted ORFs, thereby generating a non-redundant initial gene catalog [30].

Clean reads from each sample were mapped to the initial gene catalog using Bowtie2. Genes with read counts $\leq$2 across all samples were then filtered out to generate a final non-redundant gene set (Unigenes) [31]. Gene abundance for each sample was computed based on read mapping counts and gene length. This allowed for subsequent analyses, including basic statistical analyses, core-pan gene assessment, evaluation of sample correlations, and Venn diagram analysis of gene distribution.

2.6. Taxonomy Annotation

Employing the DIAMOND software (V0.9.9.110), unigenes were subjected to alignment against the sequences of bacteria, fungi, archaea, and viruses retrieved from the NCBI NR database [31]. For the finally aligned results of each sequence, as each sequence For the finally aligned results of each sequence, as each sequence might have multiple aligned results, we chose the result of which the e value $\leq 1 \times 10^{-5}$ to take the Lowest Common Ancestor (LCA) algorithm which was applied to system classification of MEGAN software to ensure the species annotation information of sequences [28].

Based on the abundance tables at each taxonomy level, Krona analysis, relative abundance overview, and abundance clustering heat map were conducted. These analyses were integrated with principal coordinate analysis (PCoA) and nonmetric multidimensional scaling (NMDS) for dimensionality reduction. Anosim analysis was a non-parametric test used to determine whether the differences between groups were significantly greater than

those within groups, thereby assessing the significance of the grouping. Metastats and Linear Discriminant Analysis (LDA) effect size (LEfSe) analysis were used to search for species differences between groups. Metastats analysis was carried out to perform a permutation test between groups at each taxonomic level and obtain a *p*-value [32]. To screen for species biomarkers with significant differences between groups, first, the rank sum test method was used to detect differentially expressed species among different groups, and then LDA was employed to reduce dimensions and evaluate the influence size of the differentially expressed species, thereby obtaining the LDA score. To ascertain the impact of the gut microbiota on the natural mating behavior of adult male giant pandas in captivity, we employed the LEfSe algorithm. This was based on the relative abundances of gut microbiota in the NM and AI groups of giant pandas. The algorithm was utilized to identify significant difference groups with LDA scores exceeding 2 [33]. It was precisely because the number of giant panda samples was limited that we adopted the method of repeated sampling from individual animals to meet the requirements of microbiome detection. However, this approach often lead to non-independent data when analyzing the differences between NM and AI groups. Additionally, the small sample size resulted in normally distributed data with unequal variances. To address this issue, we employed the Wilcoxon rank test, a non-parametric test, to compare the differences between NM and AI groups.

2.7. Common Functional Database Annotations

Unigenes were subjected to alignment against functional databases (KEGG, eggNOG, and CAZy) via DIAMOND. For each sequence, the highest-scoring match was selected to facilitate subsequent analyses [34].

The relative abundance of each functional category was computed by aggregating the relative abundances of all genes annotated to that particular category. Meanwhile, the gene counts per sample were ascertained based on non-zero abundance values among the annotated genes [28].

Based on the abundance table at each taxonomy level, annotated gene statistics were obtained. Subsequently, relative abundance overview and abundance clustering heat maps were generated. The β diversity analysis was combined with dimension reduction via PCoA and NMDS analysis, assessment of inter-and intra-group differences through Anosim analysis based on functional abundance, comparative analysis of metabolic pathways, and LEfSe analysis for identifying inter-group functional differences.

2.8. Annotations of Resistance Gene

Unigenes were aligned to the comprehensive antibiotic resistance database (CARD) database by utilizing the Resistance Gene Identifier (RGI) software (6.0.3) provided by the CARD database. The RGI software employed the built-in blastp algorithm, with a default e-value set to less than 1×10^{-30} [35].

Based on the alignment result of the RGI and the abundance information of Unigenes, the relative abundance of each ARG was computed.

Based on the abundance of ARG, various analyses were conducted, including the construction of abundance histogram, abundance clustering heat maps, and abundance distribution circular maps. Additionally, inter-group ARG differential analysis, as well as the analysis of resistance genes (Unigenes annotated as ARG) and the species attribution of resistance mechanism, were performed. (For some ARGs with lengthy names, they were abbreviated as the first three words followed by an underline). To ascertain the impact of the ARGs on the natural mating behavior of adult male giant pandas in captivity, we

employed the LEfSe algorithm. The algorithm was utilized to identify significant difference groups with LDA scores exceeding 3.

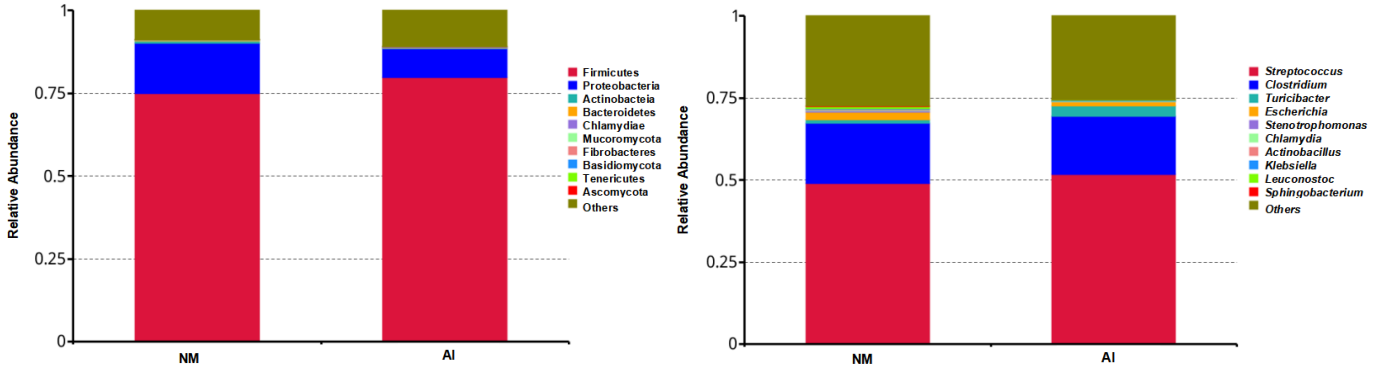
3. Results

3.1. Statistics of Raw and Effective Sequences

Following the implementation of quality control filtration, the feces of the NM and AI groups of giant pandas generated effective data of 6577.68 and 6915.30 Mbp, respectively. In the valid data, the proportion of base numbers with sequencing error rates lower than 1% (Q20) and 1 ‰ (Q30) reached 97% and 93%, respectively. This indicated a high degree of reliability in the sequencing data (Table S1). Through gene prediction, a total of 565,010 open reading frames were obtained for subsequent species annotation and gene function analysis.

3.2. Intestinal Microbiota Composition of Captive Male Adult Giant Pandas Expressing Different Natural Mating Behaviors

Figure 1 depicted the relative abundance of the top 10 microorganisms in the gut microbiota at the genus levels for captive male giant pandas in the NM and AI groups. The findings presented in Figure 1a revealed that the gut microbiota of captive adult male giant pandas in both the NM and AI groups were predominantly composed of Firmicutes, Proteobacteria, Actinobacteria, Bacteroidetes, and Chlamydiae at the phylum level. Significantly, Firmicutes and Proteobacteria were identified as the dominant phyla, together accounting for more than 85% of the total microbial community (Figure 1a). At the genus level, the top 10 species exhibiting the highest relative abundances in each sample of the NM group and the AI group were identical (Figure 1b). *Streptococcus* and *Clostridium* were recognized as the principal bacterial genera, jointly accounting for over 70% of the total microbial community (Figure 1b). Supplementary material presented the microbial composition of each sample (Figure S1).



(**a**) (**b**)

Figure 1. Histogram of relative abundance at the phylum and genus levels of Gut microbiota of captive adult male giant pandas expressing different natural mating behaviors (**a**) phylum level; (**b**) genus level. Note: In the diagram, the abscissa is organized by sample name, with each bar representing a different sample. Each taxon is distinguished by color and the ordinate represents the relative abundance of each taxon. The length of each bar corresponds to its relative abundance.

The PCoA and NMDS analysis of β diversity demonstrated that the gut microbiota of the NM group of giant pandas clustered together with that of the AI group (Figure 2; Figure S2). These experimental findings suggested that there were no significant disparities in the β diversity index (Adonis: R = 0.082, p = 0.073) of gut microbiota between the NM and AI groups.

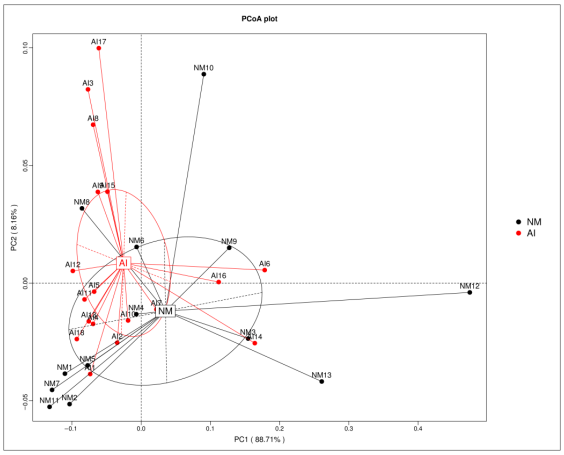


Figure 2. Cluster analysis of intestinal microbiota PCoA using Bray–Curtis dissimilarity in captive adult male giant pandas expressing different natural mating behaviors. Note: In the diagram, each data point represented a sample, and points of different colors correspond to distinct samples (groups). The proximity of two points indicates a smaller difference in species composition between the respective samples and a higher degree of similarity. The percentages enclosed in parentheses on the axes denote the proportion of variance in the raw data that can be accounted for by the principal coordinates.

3.3. Species Difference Analysis

Employing Metastats for differential microbiota analysis, we identified 315 genera and 2234 species that showed significant disparities in microbiota composition. Specifically, at the genus classification level, compared with the NM group, the AI group exhibited a relatively higher abundance of pathogenic bacterial genera and species, including the genera *Chlamydia*, *Campylobacter*, and *Helicobacter* ($p < 0.05$). In contrast, at the species level, the AI group presented an increased abundance of bacterial species associated with pathogenic bacteria, such as *Campylobacter Jejuni* and *Enterocucus Cecorum* (Figure 3). Meanwhile, the NM group demonstrated significant higher levels of non-pathogenic symbiotic bacteria, like *Clostridium* sp. *CAG306* and *Veillonella* sp. *AS16* ($p < 0.05$).

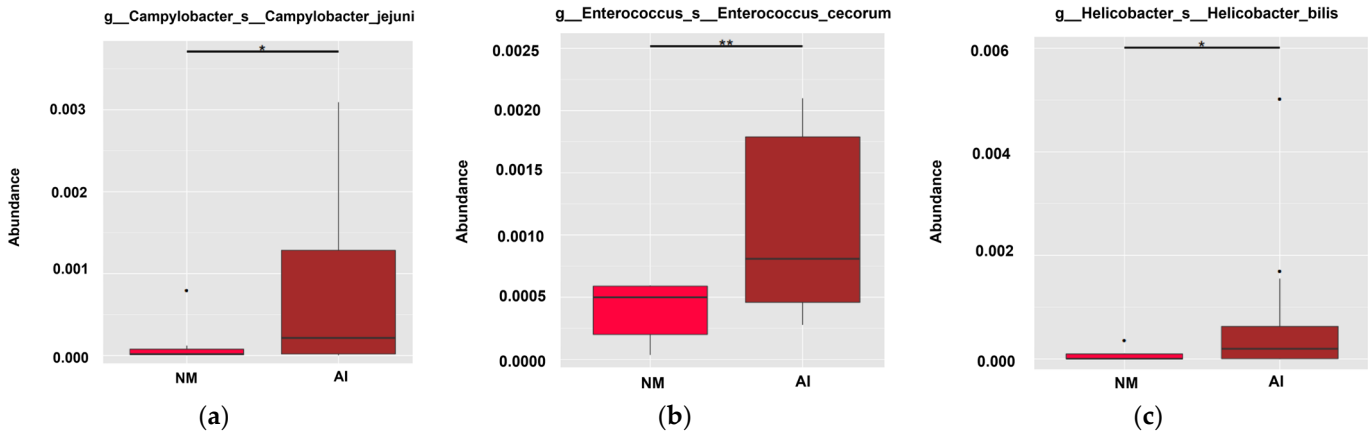


Figure 3. Bar chart display of significantly different bacterial species. Note: In the diagram, the x-axis denotes species exhibiting notable variances, while the y-axis represents the relative prevalence of said species. * $p < 0.05$; ** $p < 0.01$.

3.4. Functional Annotation and Differential Analysis of Gut Microbiota Genes in Captive Male Adult Giant Pandas Expressing Different Natural Mating Behaviors

Upon comparing the metagenomic sequencing data with functional databases (KEGG and CAZy) for functional annotation, significant differences were detected between the

NM and AI groups in metabolic pathways associated with secondary metabolite synthesis, as well as those related to sensory system, neural development, and cellular physiological regulation through LEfSe analysis. Specifically, in the AI group of giant pandas, the FoxO signaling pathway showed significant upregulation (LDA score: 2.4119; $p < 0.05$). In contrast, in the NM group of giant pandas, the olfactory transmission (LDA score: 2.5825; $p < 0.05$) and taste transmission (LDA score: 2.2568; $p < 0.05$) pathways, which were related to the sensory system, were significantly upregulated (Figure 4). A total of 126 enzyme reactions exhibited significant alterations between the two groups. Among them, 30 were specific to the AI group, including AMP deaminase [3.5.4.6] ($p < 0.01$, Wilcoxon test), while only 2 were unique to the NM group, including cellobiose hydrogenase [3.2.1.91] and allene oxide synthesis [4.2.1.92] ($p < 0.01$, Wilcoxon test); LEfSe analysis further indicated a significant enrichment of glycoside hydrolases (GH38) in the NM group (LDA score: 3.6470; $p < 0.05$), whereas glycosyltransferases (GT8) were notably enriched in the AI group (LDA score: 3.2029; $p < 0.05$) (Figure 5).

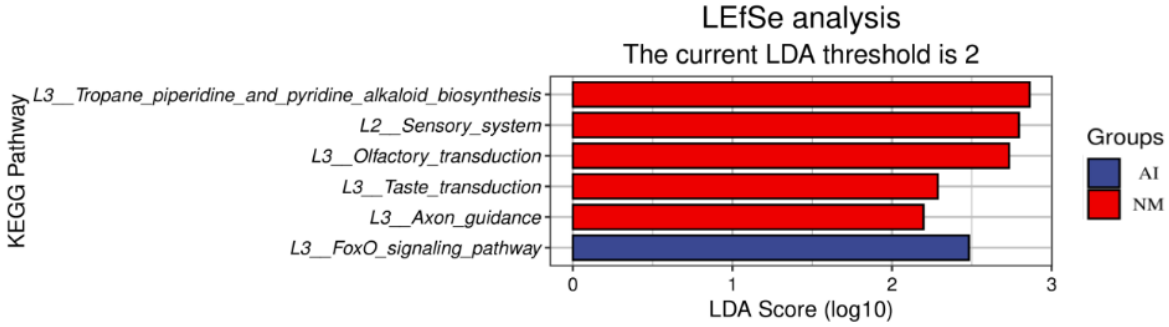
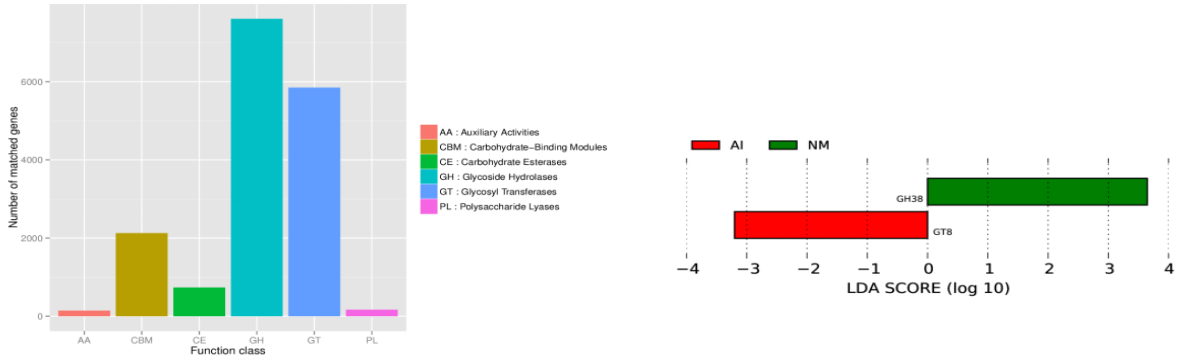


Figure 4. LEfSe functional histogram of gut microbes of captive giant pandas. Note: In the figure, the abscissa displays a bar chart visually depicting the logarithmic score value of each taxon as determined by LDA analysis. The taxa are arranged in order of their score values to illustrate their specificity within the sample grouping. Longer bars indicate greater significance of taxon differences, and the color of each bar corresponds to the most abundant sample grouping for that particular taxon.

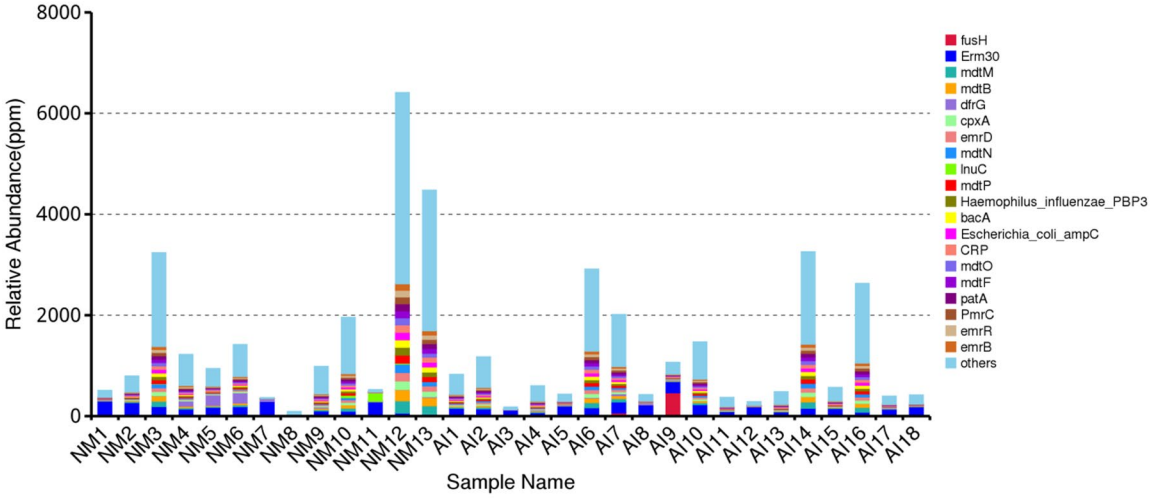


(**a**) (**b**)

Figure 5. The outcomes of comparing Unigenes with the CAZy functional database using DIAMOND software (V0.9.9.110). (**a**) Statistical chart of CAZy functional group annotation results. Notes: In the diagram, the x-axis represents each functional module of CAZy enzymes, while the y-axis indicates the number of protein families annotated to each respective module. (**b**) LDA value distribution map of differential function. Notes: The bar chart of LDA value distribution illustrates the function in which the LDA score exceeds the designated threshold (default setting is 3), indicating a biomarker with significant statistical variances among different groups. The length of each bar in the chart corresponds to the magnitude of the difference function, i.e., the LDA score.

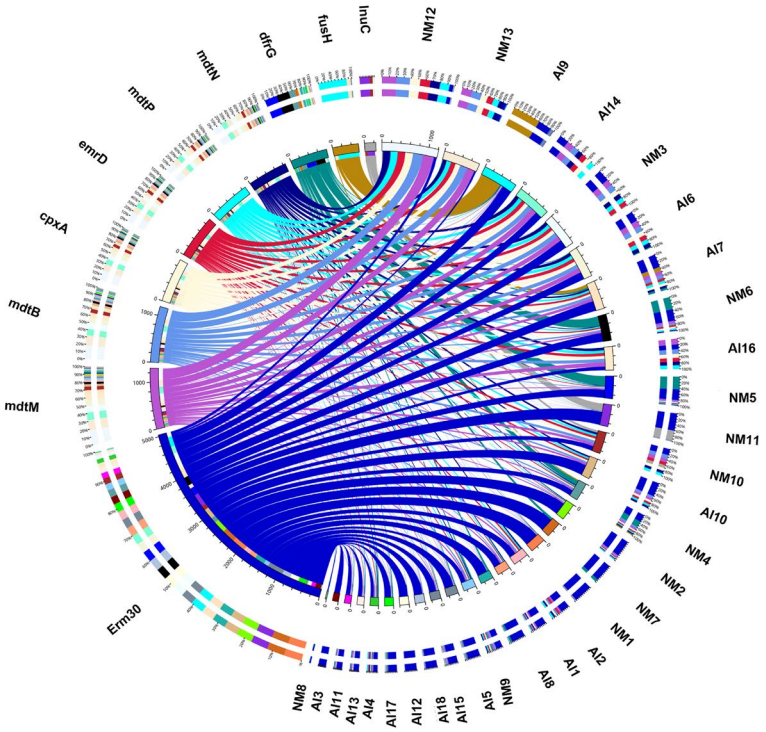
3.5. Resistance Gene Annotation

We quantified the abundance of ARGs by scaling the relative abundance of resistance genes by a factor of (10^6) times the original relative abundance data. Subsequently, the top 20 ARGs were selected for in-depth data analysis (Figure 6a,b). In both NM and AI groups, *erm30* demonstrated the highest accumulation abundance of ARGs, Proteobacteria emerged as the primary source of ARGs in both groups (Figure 6c,d). The findings of this study indicated that the proportion of macrolide and fluoroquinolone resistance genes within the gut microbiota of captive giant pandas was relatively high. No significant difference was detected in the subtype richness of resistance genes in the gut microbiota between the AI group and the NM group of giant pandas (Figure 6c,d). Furthermore, it was also observed that the composition of ARGs exhibited a more pronounced difference compared to that of the intestinal microbiota. In the NM group, the resistance gene *catII* was predominantly detected in class Gammaproteobacteria. In contrast, in the AI group, the resistance gene *norA* was mainly identified within the genus *Helicobacter* (Figure 6c,d). Our PCA-based cluster analysis unveiled significant disparities in the composition of ARGs between the NM group and the AI group (Figure 6e). Intergroup comparisons of the results indicated that the NM group exhibited a significant higher abundance of *lnuC*, *catII*, *AAC6_lai* compared to the AI group ($p < 0.05$). In contrast, the AI group displayed significantly elevated levels of *norA* and *VIM_29* relative to the NM group ($|\text{LDA score}| > 3$) ($p < 0.05$). Principal component analysis (PCA) of β−diversity revealed no significant differences in the species composition of gut microbiota between the NM group and the AI group of giant pandas (Adonis: R = 0.048, $p = 0.146$). Moreover, *tetO*, *mgtA*, and *vanD* were found to be substantially more abundant in the AI group than in the NM group (Figure 6f). These ARGs were associated with various classes of antibiotics, including fluoroquinolones, aminoglycosides, macrolides, lincosamides, tetracycline, and sulfonamides. They were also linked to carbapenemase production, as well as resistance mechanisms against phenicols and glycopeptides, encompassing antimicrobial inactivation, target protection, enhanced efflux pumps, and target replacement (Figure 6g).

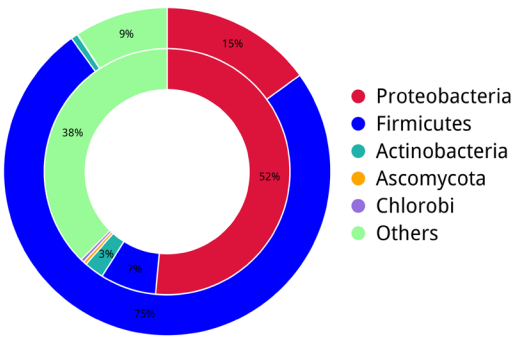


(**a**)

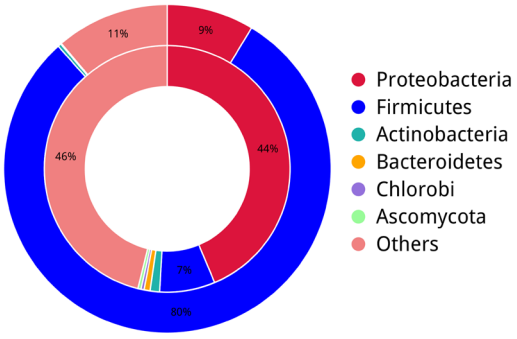
Figure 6. *Cont.*



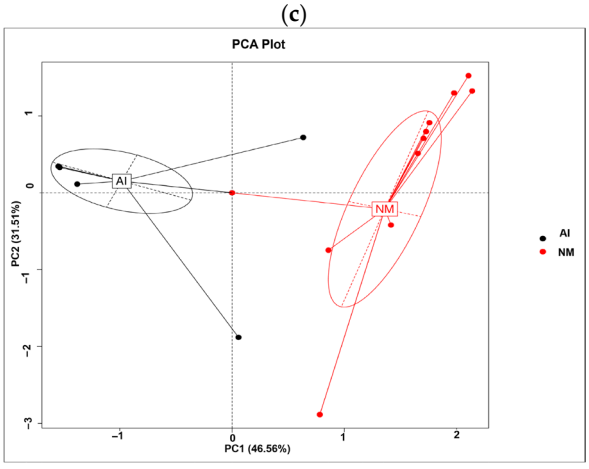
(**b**)



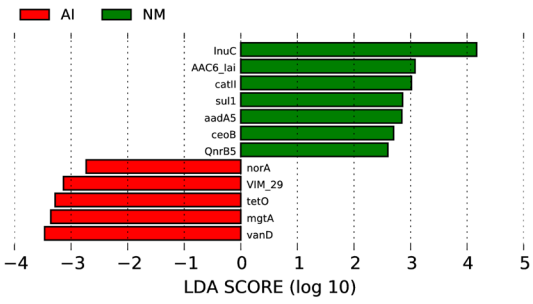
(**c**)



(**d**)

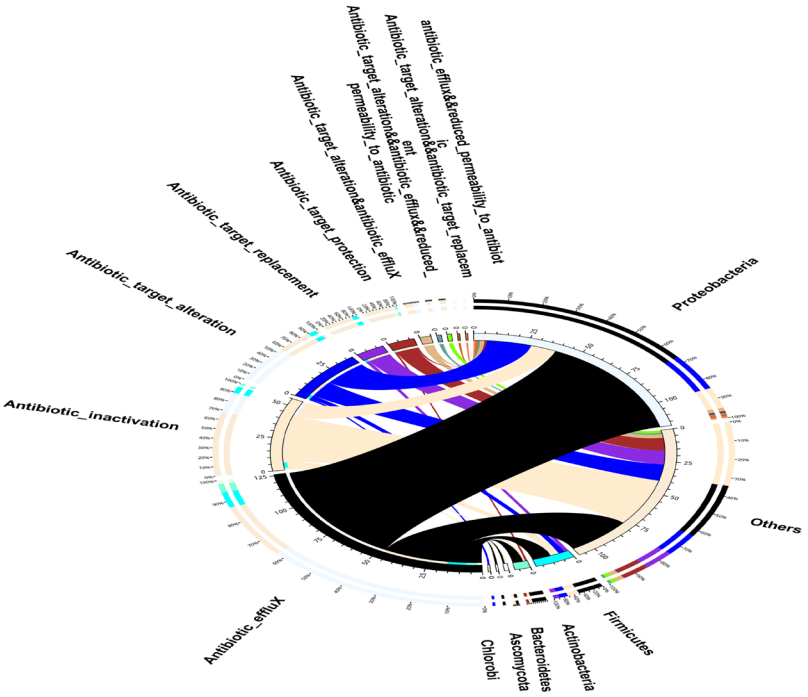


(**e**)



(**f**)

Figure 6. *Cont.*



(**g**)

Figure 6. Analysis of antibiotic resistance genes. (**a**) Abundance bar charts of different AROs in various samples; (**b**) Overview of resistance genes; Note: The circular chart is divided into two sections, with sample information displayed on the right and ARO information presented on the left. The inner circle features different colors to represent various samples and AROs, with the scale indicating their relative abundance in parts per million (ppm). The left side illustrates the total relative abundance of each ARO within a specific sample, while the right side depicts the aggregate relative abundance of each ARO across all samples. Additionally, the outer circle's left side displays the relative percentage content of each sample for a particular ARO, whereas its right side showcases the relative percentage content of each ARO within a specific sample. (**c**) Species classification analysis of antibiotic resistance genes in NM group; (**d**) Species identification analysis of antibiotic resistance genes in AI group; (**e**) PCoA diagram of intestinal microbiota; (**f**) LDA value distribution map of differential resistance genes; (**g**) Resistance mechanism and species overview loop diagram; Note: The circular chart is divided into two sections, with species information at the phylum level on the right and information about resistance mechanisms on the left. The different colors in the inner circle represent various species and resistance mechanisms, with the scale indicating the number of genes. On the left side, it shows the total number of resistance genes containing a specific type of resistance mechanism in each species, while on the right side it displays the total number of resistance genes contained in different resistance mechanisms within each species. The outer circle's left side illustrates the relative proportion of resistance genes for each species to their respective resistance mechanism's genes, whereas its right side depicts the relative proportion of resistance genes for each resistance mechanism to their respective species' resistant genes.

4. Discussion

This study attempted to utilize metagenomics technology to elucidate the relationship between the intestinal microbial community of male adult giant pandas and the resistance genes harbored within it, along with their association with mating behavior. The objective was to clarify the underlying mechanism through which the intestinal microbial community exerts an influence on mating behavior. Our study had revealed that, when compared with captive male adult giant pandas demonstrating natural expression of natural mating behavior, there was no significant variation in the β diversity of the gut microbiota of captive hosts that were unable to exhibit natural mating behavior. However, this did not rule out the possibility of changes in the

abundance of specific bacterial species. Our analysis using Metastats and LEfSe had uncovered significant differences in the relative abundances of strains and enzymes among groups. For example, the relative abundance of s_Clostridium sp. s_Veillonella sp. and f_Ruminococcaceae, which were crucial for maintaining the stability of the intestinal environment, were reduced. Conversely, the relative abundances of potential pathogenic bacteria such as s_Helicobacter pylori, which were associated with inflammation and diseases, were relatively higher in the group showing non-natural expression of natural mating behavior [36]. These findings indicated that substantial differences in gut microbiota functions, stemming from changes in the relative abundances of specific gut microbiota and the enrichment of related functional enzymes, might be primary factors influencing the natural expression of mating behavior in adult male giant pandas. Research into the intestinal microbiota had revealed that severe psychological stress can disrupt the equilibrium of the human gut flora. Such dysbiosis, driven by shifts in the taxonomic composition of the gut microbiota-particularly the *Firmicutes* to *Bacteroidetes* ratio-results in a reduction in certain microbial metabolites, such as short-chain fatty acids. This reduction subsequently impairs the brain's neurotransmitter system and exacerbates psychological stress [37]. Previous work had identified significant correlations in giant pandas between fecal levels of Clostridium tetani and s_Clostridium_sp_MSJ_8 and the synthesis of the short-chain fatty acid propionate and its metabolite methylmalonate [38]. Importantly, psychological stress induced by suboptimal captive environments has been established as a critical factor disrupting the natural mating behavior of giant pandas [16,39]. Furthermore, the analysis of resistance genes unveiled the existence of diverse resistance gene types within the intestinal microbiota of captive adult giant pandas. This phenomenon could be ascribed to the utilization of antibiotics such as tetracycline and macrolide during the feeding and management phases of the captive giant panda population under investigation in this study. The notable disparities in the relative abundance of resistance genes across groups suggested that distinct categories of gut microbiota resistance genes could be associated with the manifestation of natural mating behavior in captive adult male giant pandas (Notably, the upregulated resistance genes in the NM group mainly consist of lincosamide antibiotic, aminoglycoside antibiotic, and sulfonamide antibiotic, whereas those in the AI group predominantly comprised macrolide antibiotic, glycopeptide antibiotic, and tetracycline antibiotic). The gut microbiota constituted a significant reservoir of ARGs, with notable correlations observed among ARG compositions. Previous research had indicated that inappropriate antibiotic use can alter the composition and abundance of the host gut microbiota [5]. Our study revealed substantial differences in the ARG profiles of gut microbiomes between giant pandas exhibiting natural mating behavior and those displaying non-natural mating behavior. Such alterations might disrupt sex pheromone synthesis, ultimately contributing to impaired mate selection and aberrant mating behavior [40]. Analysis of the intestinal microbiota of captive adult male giant pandas with differing natural mating capacities further demonstrated that an imbalance in microbial abundance, characterized by the enrichment of potentially pathogenic bacteria such as s_Helicobacter pylori, might represent a key fecal microbiota biomarker. Correlations between intestinal microbiota and ARGs indicated that in males incapable of natural mating, s_Helicobacter pylori and other harmful bacteria acted as principal reservoirs of ARGs. These findings suggested that an increased abundance of detrimental gut bacteria might be linked to the accumulation of ARGs, possibly resulting from routine antibiotic administration.

Simultaneously, the kegg pathway annotation and functional prediction results further indicated that metabolic pathways related to sensory systems, such as taste and olfactory transduction, were significantly upregulated in the intestines of captive adult male giant pandas demonstrating natural mating behavior ($|\text{LDA score}| > 2$, $p < 0.05$). This discovery suggested that modifications in the abundance of gut microbiota might influence the synthesis and reception of chemical signals in giant pandas. Such influences could lead to unsuccessful

mate selection and ultimately result in aberrant expression of natural mating behavior. Previous investigations had demonstrated that the giant panda, a wild species, utilizes symbiotic bacteria within its glands to engage in the synthesis of host chemical signal substances [41]. Notably, there existed substantial disparities in the microbiome between giant pandas with robust reproductive capabilities and those with relatively weak reproductive capacities. Male giant pandas capable of successful natural mating exhibited elevated levels of Clostridium [42]. Research into the role of sex hormones in mammalian mating behavior had continued to advance. Previous studies had revealed that gut microbiota modulate sexual attractiveness and mating preferences in mammals by influencing individual-specific odors mediated by sex pheromones. Their work suggests that gut microbiota alter the abundance of these odorant pheromones, which in turn shapes the mating decisions of animals [4]. Our prior research had also revealed that microorganisms such as Veillonellaceae and Lactobacillaceae, along with key enzymes like acetate kinase and pyruvate oxidase in the intestinal tract of captive adult male giant pandas, were implicated in the synthesis of volatile metabolites, including acetic acid. This, in turn, influenced mate selection and the manifestation of natural mating behavior [24]. We therefore hypothesized that alterations in the gut microbiota are driven by environmental factors such as antibiotic administration, which might promote the enrichment of ARGs and could facilitate the production of key chemical signaling molecules in the perianal glands via microbial metabolites. Alternatively, microbial-derived short-chain fatty acids and other metabolites might influence giant panda neurodevelopment and psychological states through the gut–brain axis, ultimately disrupting natural communication and mating behavior [43]. The findings of this study offered a novel augmentation to the theory that the intestinal microbiota impacted the expression of natural mating behavior in giant pandas.

5. Conclusions

Nevertheless, the present findings, which relied exclusively on fecal microbiome data, remained speculative in the absence of validation via targeted metabolomic profiling or neurophysiological evaluations. Furthermore, constraints imposed by the endangered status of giant pandas and ethical considerations resulted in a limited sample size. Future studies employing multi-omics methodologies and larger cohorts would be necessary to corroborate these initial observations.

This study presented the initial evidence suggesting that the changes in the abundance of gut microbiota and resistance genes might be associated with the manifestation of natural mating behavior in captive adult male giant pandas. The findings of this study offered novel perspectives on how the captive environment influenced the decline in natural mating behavior among adult male giant pandas.

Supplementary Materials: The following supporting information can be downloaded at: https://www.mdpi.com/article/10.3390/microbiolres17020043/s1, Figure S1: Histogram of relative abundance at the phylum and genus levels of gut microbiota of captive adult male giant pandas expressing different natural mating behaviors; Figure S2: Dimensionality reduction analysis based on species abundance using Non-Metric Multi-Dimensional Scaling; Table S1: Data preprocessing statistics.

Author Contributions: Conceptualization, M.-Y.Z.; Y.-L.L. and R.H.; methodology, M.-Y.Z.; X.-H.Z. and X.-Y.W.; software, X.-H.Z. and X.-Y.W.; validation, X.-H.Z.; formal analysis, X.-H.Z. and X.-Y.W.; resources, M.-Y.Z.; Y.-L.L. and R.H.; data curation, J.-H.A.; and D.-H.W.; Writing—original draft preparation, X.-H.Z.; writing—review and editing, M.-Y.Z.; visualization, M.-Y.Z.; supervision, Y.-L.L. and R.H.; project administration, M.-Y.Z. and Y.-L.L. All authors have read and agreed to the published version of the manuscript.

Funding: This research was funded by the Program of the Chengdu Research Base of Giant Panda Breeding (2024CPB-B15 and CAZG2025B09).

Institutional Review Board Statement: The study was conducted in accordance with the Animal Management and Use Committee of the Chengdu Giant Panda Breeding Research Base (Approval No.: 2020013) (Approval date: 19 May 2020). All experiments were performed in accordance with relevant guidelines and regulations.

Informed Consent Statement: Not applicable.

Data Availability Statement: The datasets generated for this study can be found in the NCBI (https://www.ncbi.nlm.nih.gov/bioproject/PRJNA1035989/) (Published date: 1 December 2024), PRJNA1035989.

Acknowledgments: We greatly appreciate the assistance provided by the staff at the Chengdu Research Base of Giant Panda Breeding. We also acknowledge Novogene for conducting the metagenomics analysis.

Conflicts of Interest: The funders had no role in the design of the study; in the collection, analyses, or interpretation of data; in the writing of the manuscript; or in the decision to publish the results.

References

1. Wu, W.L.; Adame, M.D.; Liou, C.W.; Barlow, J.T.; Lai, T.T.; Sharon, G.; Schretter, C.E.; Needham, B.D.; Wang, M.I.; Tang, W.; et al. Microbiota regulate social behaviour via stress response neurons in the brain. *Nature* **2021**, *595*, 409–414. [CrossRef]
2. Dalile, B.; Van Oudenhove, L.; Vervliet, B.; Verbeke, K. The role of short-chain fatty acids in microbiota-gut-brain communication. *Nat. Rev. Gastroenterol. Hepatol.* **2019**, *16*, 461–478. [CrossRef]
3. Foster, J.A.; Rinaman, L.; Cryan, J.F. Stress & the gut-brain axis: Regulation by the microbiome. *Neurobiol. Stress* **2017**, *7*, 124–136. [CrossRef]
4. Yi, X.; Cha, M. Gut Dysbiosis Has the Potential to Reduce the Sexual Attractiveness of Mouse Female. *Front. Microbiol.* **2022**, *13*, 916766. [CrossRef]
5. Huang, G.P.; Qu, Q.Y.; Wang, M.; Huang, M.P.; Zhou, W.L.; Wei, F.W. Global landscape of gut microbiome diversity and antibiotic resistomes across vertebrates. *Sci. Total Environ.* **2022**, *838*, 156178. [CrossRef] [PubMed]
6. Chen, F.F.; Di, H.X.; Lan, L.F. Small molecules targeting Staphylococcus aureus virulence. *Chin. Sci. Bull.* **2013**, *58*, 3743–3752. (In Chinese) [CrossRef]
7. Yan, Z.; Yao, Y.; Xu, Q.; He, X.; Zhou, X.Y.; Wang, H.R. Dietary microbiota-mediated shifts in gut microbial ecology and pathogen interactions in giant pandas (*Ailuropoda melanoleuca*). *Commun. Biol.* **2025**, *8*, 864. [CrossRef]
8. Cryan, J.F.; O'Riordan, K.J.; Cowan, C.S.M.; Sandhu, K.V.; Bastiaanssen, T.F.S.; Boehme, M.; Codagnone, M.G.; Cussotto, S.; Fulling, C.; Golubeva, A.V.; et al. The Microbiota-Gut-Brain Axis. *Physiol. Rev.* **2019**, *99*, 1877–2013. [CrossRef] [PubMed]
9. Sherwin, E.; Bordenstein, S.R.; Quinn, J.L.; Dinan, T.G.; Cryan, J.F. Microbiota and the social brain. *Science* **2019**, *366*, eaar2016. [CrossRef] [PubMed]
10. Francino, M.P. Antibiotics and the human gut microbiota: Dysbioses and accumulation of resistances. *Front. Microbiol.* **2016**, *6*, 1543. [CrossRef]
11. Pérez-Cobas, A.E.; Gosalbes, M.J.; Friedrichs, A.; Knecht, H.; Artacho, A.; Eismann, K.; Otto, W.; Rojo, D.; Bargiela, R.; von Bergen, M.; et al. Gut microbiota disturbance during antibiotic therapy: A multi-omic approach. *Gut* **2013**, *62*, 1591–1601. [CrossRef]
12. Zhang, Q.Y.; Cheng, L.; Wang, J.J.; Hao, M.Z.; Che, H.L. Antibiotic-Induced Gut Microbiota Dysbiosis Damages the Intestinal Barrier, Increasing Food Allergy in Adult Mice. *Nutrients* **2021**, *13*, 3315. [CrossRef]
13. Conde, D.A.; Flesness, N.; Colchero, F.; Jones, O.; Scheuerlein, A. An emerging role of zoos to conserve biodiversity. *Science* **2011**, *331*, 1390–1391. [CrossRef] [PubMed]
14. Simberloff, D. Flagships, umbrellas, and keystones: Is single species management passé in the landscape era. *Biol. Conserv.* **1998**, *83*, 247–257. [CrossRef]
15. Xie, Z. *The 2016 International Studbook for Giant Panda (Ailuropoda melanoleuca)*; Bristol Zoo Gardens: Bristol, UK, 2016.
16. Zhang, M.Y.; Wang, X.Y.; Zhang, X.H.; Hou, R. Urine metabolomics reveals the effects of confined environment on mating choice in adult male giant pandas. *Physiol. Behav.* **2022**, *249*, 113744. [CrossRef] [PubMed]
17. Zhang, M.Y.; Zhang, X.H.; Zhang, P.; Liu, Y.L.; Hou, R. Natural reproductive performance is associated with captive management in adult male giant pandas. *Appl. Anim. Behav. Sci.* **2021**, *240*, 105353. [CrossRef]
18. Schaller, G.B.; Hu, J.C.; Pan, W.S.; Zhu, J. *The Giant Pandas of Wolong*; University Of Chicago Press: Chicago, IL, USA, 1985.
19. Owen, M.A.; Swaisgood, R.R.; Zhou, X.; Blumstein, D.T. Signalling behaviour is influenced by transient social context in a spontaneously ovulating mammal. *Anim. Behav.* **2016**, *111*, 157–165. [CrossRef]

20. Martin-Wintle, M.S.; Shepherdson, D.; Zhang, G.Q.; Zhang, H.M.; Li, D.S.; Zhou, X.P.; Li, R.G.; Swaisgood, R.R. Free mate choice enhances conservation breeding in the endangered giant panda. *Nat. Commun.* **2015**, *610*, 125. [CrossRef]
21. Swaisgood, R.R.; Lindburg, D.G.; White, A.M.; Zhang, H.M.; Zhou, X.P. *Chemical Communication in Giant Pandas: Experimentation and Application*; Lindburg, D.B.K., Ed.; University of California Press: Berkeley, CA, 2004; pp. 106–120.
22. Charlton, B.D.; Keating, J.L.; Huang, Y.; Li, R.G.; Swaisgood, R.R. Female giant panda (*Ailuropoda melanoleuca*) chirps advertise the caller's fertile phase. *Proc. Roy. Soc. Lond. B* **2010**, *277*, 1101–1106. [CrossRef]
23. Stewart, C.J.; Ajami, N.J.; O'Brien, J.L.; Hutchinson, D.S.; Smith, D.P.; Wong, M.C.; Ross, M.C.; Lloyd, R.E.; Doddapaneni, H.; Metcalf, G.A.; et al. Temporal development of the gut microbiome in early childhood from the TEDDY study. *Nature* **2018**, *562*, 583–588. [CrossRef]
24. Zhang, M.Y.; Zhang, X.H.; Wang, X.Y.; Liu, Y.L.; An, J.H.; Wang, D.H.; Cai, Z.G.; Hou, R. Intestinal acetic acid regulates the synthesis of sex pheromones in captive giant pandas. *Front. Microbiol.* **2023**, *14*, 1234676. [CrossRef]
25. Karlsson, F.H.; Tremaroli, V.; Nookaew, I.; Bergström, G.; Behre, C.J.; Fagerberg, B.; Nielsen, J.; Bäckhed, F. Gutmetagenome in European women with normal, impaired and diabetic glucose control. *Nature* **2013**, *498*, 99–103. [CrossRef]
26. Nielsen, H.B.; Almeida, M.; Juncker, A.S.; Rasmussen, S.; Li, J.; Sunagawa, S.; Plichta, D.R.; Gautier, L.; Pedersen, A.G.; Le Chatelier, E.; et al. MetaHIT Consortium. Identification and assembly of genomes and genetic elements in complex metagenomic samples without using reference genomes. *Nat. Biotechnol.* **2014**, *32*, 822–828. [CrossRef]
27. Qin, J.J.; Li, R.; Raes, J.; Arumugam, M.; Burgdorf, K.S.; Manichanh, C.; Nielsen, T.; Pons, N.; Levenez, F.; Yamada, T.; et al. A human gut microbial gene catalogue established by metagenomic sequencing. *Nature* **2010**, *464*, 59–65. [CrossRef]
28. Karlsson, F.H.; Fåk, F.; Nookaew, I.; Tremaroli, V.; Fagerberg, B.; Petranovic, D.; Bäckhed, F.; Nielsen, J. Symptomatic atherosclerosis is associated with an altered gut metagenome. *Nat. Commun.* **2012**, *3*, 1245. [CrossRef]
29. Sunagawa, S.; Coelho, L.P.; Chaffron, S.; Kultima, J.R.; Labadie, K.; Salazar, G.; Djahanschiri, B.; Zeller, G.; Mende, D.R.; Alberti, A.; et al. Ocean plankton. Structure and function of the global ocean microbiome. *Science* **2015**, *348*, 1261359. [CrossRef] [PubMed]
30. Fu, L.M.; Niu, B.F.; Zhu, Z.W.; Wu, S.T.; Li, W.Z. CD-HIT: Accelerated for clustering the next-generation sequencing data. *Bioinformatics* **2012**, *28*, 3150–3152. [CrossRef] [PubMed]
31. Buchfink, B.; Xie, C.; Huson, D.H. Fast and sensitive protein alignment using DIAMOND. *Nat. Methods* **2015**, *12*, 59–60. [CrossRef]
32. White, J.R.; Nagarajan, N.; Pop, M. Statistical methods for detecting differentially abundant features in clinical metagenomic samples. *PLoS Comput. Biol.* **2009**, *5*, e1000352. [CrossRef]
33. Segata, N.; Izard, J.; Waldron, L.; Gevers, D.; Miropolsky, L.; Garrett, W.S.; Huttenhower, C. Metagenomic biomarker discovery and explanation. *Genome Biol.* **2011**, *12*, R60. [CrossRef] [PubMed]
34. Qin, J.J.; Li, Y.R.; Cai, Z.M.; Li, S.H.; Zhu, J.F.; Zhang, F.; Liang, S.S.; Zhang, W.W.; Guan, Y.L.; Shen, D.Q.; et al. A metagenome-wide association study of gut microbiota in type 2 diabetes. *Nature* **2012**, *490*, 55–60. [CrossRef]
35. Martínez, J.L.; Coque, T.M.; Baquero, F. What is a resistance gene? Ranking risk in resistomes. *Nat. Rev. Microbiol.* **2014**, *13*, 116–123. [CrossRef] [PubMed]
36. Hu, W.; Chen, Z.M.; Wang, Y.; Yang, C.; Wu, Z.Y.; You, L.J.; Zhai, Z.Y.; Huang, Z.Y.; Zhou, P.; Huang, S.L.; et al. Single-cell RNA sequencing dissects the immunosuppressive signatures in Helicobacter pylori-infected human gastric ecosystem. *Nat. Commun.* **2025**, *16*, 3903. [CrossRef] [PubMed]
37. Valles-Colomer, M.; Falony, G.; Darzi, Y.; Tigchelaar, E.F.; Wang, J.; Tito, R.Y.; Schiweck, C.; Kurilshikov, A.; Joossens, M.; Wijmenga, C.; et al. The neuroactive potential of the human gut microbiota in quality of life and depression. *Nat. Microbiol.* **2019**, *4*, 623–632. [CrossRef]
38. Zhang, X.H.; Wang, X.Y.; Ayala, J.; Liu, Y.L.; An, J.H.; Wang, D.H.; Cai, Z.G.; Hou, R.; Zhang, M.Y. Possible effects of early maternal separation on the gut microbiota of captive adult giant pandas. *Animals* **2022**, *12*, 2587. [CrossRef]
39. Wang, X.Y.; Yuan, B.; Huang, H.; Zhang, X.H.; Liu, Y.L.; Hou, R.; Zhang, M.Y. Abnormal expression of natural mating behaviour of captive adult giant pandas is related to physiological stress. *Conserv. Physiol.* **2024**, *12*, coae061. [CrossRef]
40. Ren, L.; Ma, Y.G.; Xie, M.X.; Lu, Y.Y.; Cheng, D.F. Rectal bacteria produce sex pheromones in the male oriental fruit fly. *Curr. Biol.* **2021**, *31*, 2220–2226.e4. [CrossRef]
41. Zhou, W.L.; Qi, D.W.; Swaisgood, R.R.; Wang, L.; Jin, Y.; Wu, Q.; Wei, F.W.; Nie, Y.G. Symbiotic bacteria mediate volatile chemical signal synthesis in a large solitary mammal species. *ISME J.* **2021**, *15*, 2070–2080. [CrossRef] [PubMed]
42. Yan, Z.; Lei, Y.H.; Zhao, P.P.; Zhang, D.H.; Shen, J.N.; Zhang, G.Q.; Wei, R.P.; Liu, H.Q.; Liu, X.Y.; He, Y.; et al. Natural mating ability is associated with gut microbiota composition and function in captive male giant pandas. *Ecol. Evol.* **2024**, *14*, e11189. [CrossRef]
43. Theis, K.R.; Venkataraman, A.; Dycus, J.A.; Koonter, K.D.; Schmitt-Matzen, E.N.; Wagner, A.P.; Holekamp, K.E.; Schmidt, T.M. Symbiotic bacteria appear to mediate hyena social odors. *Proc. Natl. Acad. Sci. USA* **2013**, *110*, 19832–19837. [CrossRef]

Disclaimer/Publisher's Note: The statements, opinions and data contained in all publications are solely those of the individual author(s) and contributor(s) and not of MDPI and/or the editor(s). MDPI and/or the editor(s) disclaim responsibility for any injury to people or property resulting from any ideas, methods, instructions or products referred to in the content.